Talanta 89 (2012) 253–257

Contents lists available at SciVerse ScienceDirect

Talanta

journal homepage: www.elsevier.com/locate/talanta

Selective discrimination of small hydrophobic biomolecules based on ion-current rectification in conically shaped nanochannel

Zhijun Guo, Jiahai Wang*, Erkang Wang*

State Key Laboratory of Electroanalytical Chemistry, Changchun Institute of Applied Chemistry, Chinese Academy of Sciences, Changchun, Jilin 130022, China

ARTICLE INFO

Article history:
Received 8 September 2011
Received in revised form 6 December 2011
Accepted 10 December 2011
Available online 14 December 2011

Keywords:
Ion current rectification
Conically shaped nanochannel
Biomimetic
Polymer membrane
Sensors
Small hydrophobic biomolecules

ABSTRACT

In this study, based on ion-current rectification in the conically shaped nanochannel embedded in polyethylene terephthalate (PET) membrane, we have selectively discriminated three small biomolecules. Because three positive biomolecules (Hoechst 33342, Propidium and Bupivacaine) have different hydrophobicities, their interactions with inside wall of the conical nanochannel are different and their binding affinities can be derived from Langmuir absorption model. Therefore, we can successfully discriminate these small biomolecules. The highest binding constant was obtained for the small molecule with highest hydrophobicity. Another interesting result is that the detection limit for the small molecule with the highest binding constant shifts to submicromole.

1. Introduction

Synthetic nanochannels [1–27] embedded in polymer membrane have attracted great attention due to their facile fabrication and easy functionalization. As an alternative to biological counterpart [28–31], nanochannel in solid-state film can be adjusted to various nanochannel sizes, which is extremely important for selective detection of specific target. Until now, there are two basic methods for target analysis via conically shaped nanochannel: resistive-pulse sensing [3,4] and ion-current rectification [12,27].

Comparatively, biosensor based on ion-current rectification is much less sensitive to the physical properties of nanochannel tip than resisitive-pulse sensing. The sensor element in this case is a single conically shaped nanochannel in a polyethylene terephthalate membrane [11]. The sensing paradigm entails placing electrolyte solutions on either side of the membrane and using electrodes in each solution to scan the applied transmembrane potential and measure the resulting ion current flowing through the nanochannel. As has been discussed in detail by others [3,4,6,7,9,10,32–35], conically shaped nanochannels with excess surface charge on the pore walls, and sufficiently small tip openings, show non-linear current voltage curves; *i.e.*, such pores possess ion-current rectifying ability. Because the nanochannels in PET used here have excess anionic surface charge, rectification is observed at applied transmembrane potentials [27].

It has been reported [27] previously that when the nanochannel is exposed to a very hydrophobic, yet cationic small molecule, adsorption of this molecule on the pore walls of polyimide (Kapton) neutralizes the excess negative surface charge. Inspired by this interesting discovery, we are seeking to explore whether nanochannel fabricated from other polymer material can selectively discriminate different small hydrophobic biomolecules due to their inherent hydrophobicity. PET materials were selected to fabricate conically shaped nanochannel because of its easy fabrication as compared to Kapton membrane. Here, by choosing Hoechst 33342, Propidium iodide and Bupivacaine as typical examples, we demonstrated the conically shaped nanochannel embedded in PET membrane can be used to selectively discriminate cationic hydrophobic biomolecules by utilization of ion-current rectification. Hoechst 33342 is much more hydrophobic and Propidium iodide and Bupivacaine are less hydrophobic. The reason why we choose these molecules is because that Hoechst 33342 has similar planar structure as Hoechst 33328, which can help us to better understand the mechanism behind the absorption of small molecules onto the membrane. Furthermore, these positive molecules have significant difference in hydrophobicity and the structures of these molecules have different level of planarity which may clarify the role of aromatic stacking interaction.

* Corresponding authors. Tel.: +86 431 85262003; fax: +86 431 85689711.
E-mail addresses: jhwang@ciac.jl.cn (J. Wang), ekwang@ciac.jl.cn (E. Wang).

0039-9140/$ – see front matter © 2011 Elsevier B.V. All rights reserved.
doi:10.1016/j.talanta.2011.12.022

2. Experimental

2.1. Chemicals and materials

PET (poly(ethylene terephthalate)) membranes (diameter = 3 cm, thickness = 12 μm) that had been irradiated with a heavy ion of 2.2 GeV kinetic energy to create a single damage track through the membrane were obtained from GSI, Darmstadt, Germany and referred to as the "tracked" membranes. The surfactant DOWfax 2A1 was purchased from DOW Chemical. Sodium chloride (NaCl) and potassium chloride (KCl) were purchased from Beijing Chemical Reagent Company (Beijing, China). Hoechst 33342, Propidium iodide, Bupivacaine (Fig. 1) were purchased from Sigma–Aldrich and used as received. Tris–HCl used to prepare the buffer solutions, was also obtained from Aldrich. All of the chemicals were of at least analytical grade. Purified water was prepared by passing house-distilled water through a Millipore Milli-Q water purification system.

2.2. Fabrication of asymmetrical nanochannel

Each side of the tracked PET membrane was irradiated under UV light (365 nm) for 1 h, and then the membrane was mounted in a two-compartment cell such that electrolyte solution could be placed on either side of the tracked membrane. The temperature during etching was maintained at 40 °C. Each half cell contained a Pt wire (dia = 0.1 cm, length ~ 5 cm), and a Keithley 2536A picoammeter/voltage-source (Keithley Instruments, Cleveland, OH) was used to apply a transmembrane potential of 1 V during etching and measure the resulting current ionic flowing through the nascent nanochannel. Nanochannels with the tip diameter of 22 nm was fabricated with surfactant-protected one-step etching method described by Ali for preparing conically shaped nanochannels in tracked poly(ethylene terephthalate) membranes [36]. Protecting solution (6 M NaOH + 0.07% 2A1) was placed on one side of the membrane, 6 M sodium hydroxide solution was placed on the UV-treated side to control the diameter of big opening of the nanochannel. When desired current was reached, 1 M HCl solution was placed on both side of the membrane to stop the etching process. According to previous procedure [36], the diameter of the base opening was determined by obtaining scanning electron micrographs of the base side of multi-tracked PET membranes (1×10^8 tracks cm^{-2}) etched under the same conditions (Fig. 2A).

The tip diameter (d) after the second etching was measured using the electrochemical method described in detail previously [37,38]. The following equation was used to calculate tip diameter:

$$d = \frac{4LI}{\pi DkV}$$

where L is the membrane thickness, k is the conductivity of the electrolyte, V is the transmembrane voltage, and I is the ionic current. The equation provides a solution to obtain the tip diameter of ideal conically shaped nanochannel. However, the tip diameter cannot be directly imaged by current techniques; therefore, a rough estimation of tip diameter has to be used.

2.3. Sensing the analyte biomolecules

The membrane containing the conically shaped nanochannel was mounted in the two-compartment cell, and a solution containing the desired analyte molecule (Fig. 1) was placed in the compartment facing the tip opening of the membrane. This solution was prepared in 10 mM Tris buffer (pH = 7.0) containing 100 mM KCl, and the same buffer solution, devoid of the analyte, was placed on the opposite side of the membrane. Ag/AgCl electrode was placed into each solution, and the Keithley 2536A was used to obtain a current–voltage (I–V) curve associated with ion transport through the nanochannel. The working Ag/AgCl electrode was in the half-cell facing the base opening, and the potential of this electrode was controlled relative to the counter Ag/AgCl electrode in the opposite solution. The I–V curve was obtained by scanning the potential from −2 V to +2 V.

3. Results and discussion

3.1. Selection of proper polymer material for fabrication of conically shaped nanochannel

Among those investigations focusing on nanochannels in polymer membranes [1,8,9,18,20,24,39], PET membrane has been used to investigate physical foundation of ion transport across biomimetic nanochannel embedded in the membrane due to its dramatic advantages as compared to others. Firstly, etching heavy ion track in the PET membrane only entails placing sodium hydroxide either on one side [38] or on both sides of the membrane [36]. Secondly, the small opening of the nanochannel can be adjusted at will by stopping the etching process at desired current value, which can be used to estimate the tip size of conically shaped nanochannel. Finally, the surface of PET after etching using high concentration of sodium hydroxide is ended with carboxyl group, which facilitates further functionalization of the inner channel wall. In combination with other various tools, various methods have been reported to chemically modify the surface wall of nanochannel to tune the ion transport.

3.2. Ion-current rectification by conical nanochannel

As shown in Fig. 3A (Figs. 4A and 5A), I–V curves for a conical nanochannel in a PET membrane with and without the analyte demonstrate dramatic difference. In the absence of these small molecules, the I–V curves are non-linear, indicating that the nanochannel with negative surface charge strongly rectifies the ion current flowing through it [7,10,12,24]. Several comprehensive simulations [7,8] have been accomplished to explain the ion current rectification. Ion current rectification through conically shaped nanopore requires that surface charge density is asymmetrically distributed along the nanochannel and the diameter of the tip opening is in proper relationship with the thickness of the electrical double layer extending from the pore wall.

The ion-current rectification phenomenon can be described by defining "on" and "off" states for the nanochannel rectifier [40]. Figs. 3A, 4A and 5A show that in the absence of each analyte, the "on" state occurs at negative potentials and the "off" state at positive potentials. These indicate that rectification is caused by fixed anionic (carboxylate) groups on the pore wall. The extent of rectification can be quantified by the rectification ratio defined here as the absolute current at −2.0 V divided by the absolute current at +2.0 V (Fig. 2B).

3.3. Effect of three cationic hydrophobic biomolecules on rectification

Several key observations reproduced by Hoechst 33342 are the followings: as Hoechst 33342 is added, the extent of rectification decreases (Fig. 3A); the extent of rectification scales inversely with the concentration of Hoechst 33342 (Table 1); ultimately at high small molecule concentrations, the rectification is reversed (Fig. 3A). This reversal in rectification is signaled by the fact that at high small molecule concentrations the "on" state is at

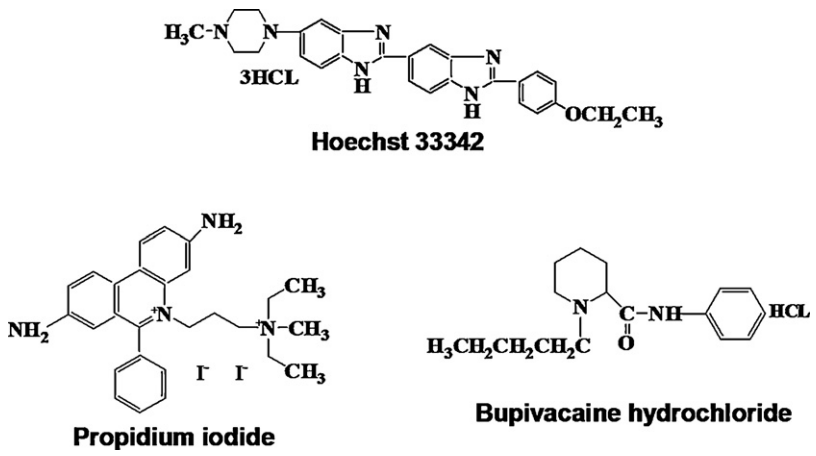

Fig. 1. Molecular structure of small biomolecules.

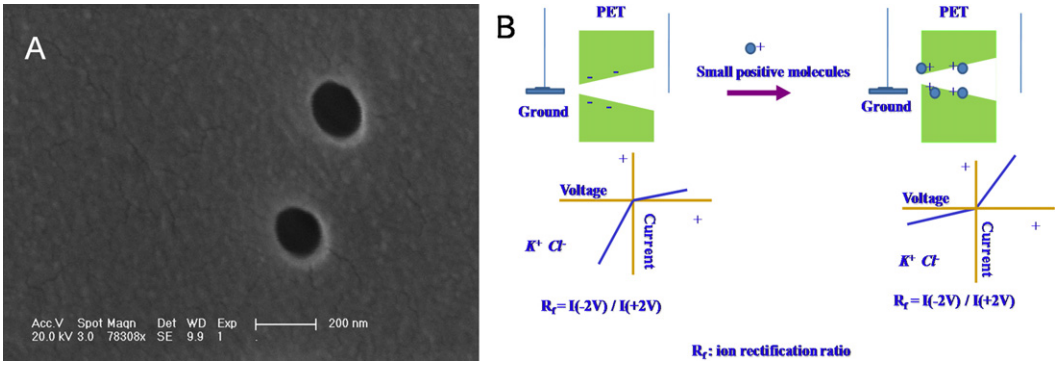

Fig. 2. Scanning electron micrograph of multipore etched in PET polymer under the same etching conditions as that for single-tracked nanochannel.

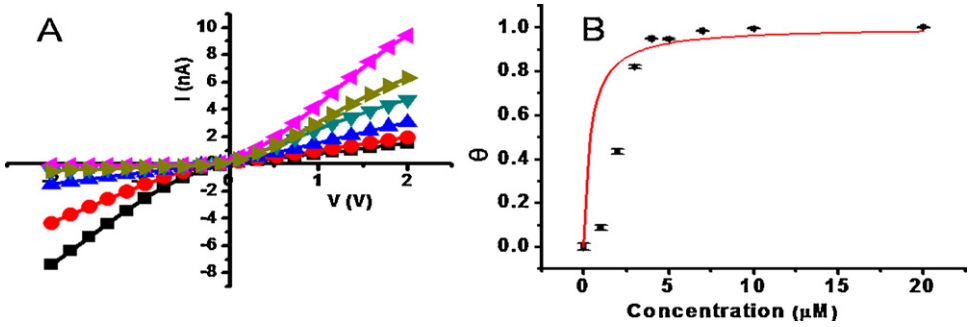

Fig. 3. (A) *I–V* curves for a conical nanochannel sensor (tip diameter = 22 nm, base diameter 200 nm) in the presence of the following concentrations of Hoechst 33342: 0 nM (black square), 2 μM (red circle), 3 μM (blue triangle), 4 μM (green triangle), 5 μM (dark yellow triangle), 20 μM (pink triangle). (B) Plot of surface coverage (theta) versus concentration of Hoechst 33342. Red line is the fitting curve. Experimental conditions: 10 mM Tris buffer (pH = 7.0) with 100 mM in KCl; Error bar from three experimental measurements. (For interpretation of the references to color in this figure legend, the reader is referred to the web version of the article.)

positive potentials and the "off" state is at negative potentials. High small molecule concentration drives the rectification ratio to be less than unity (Table 1). Reversal of ion current rectification also indicates that the membrane becomes positively charged due to excess adsorption of cationic small biomolecule. As compared to Hoechst 33342, the change of ion current rectification in presence of other two small biomolecules (Propidium and Bupivacaine) has similarity and dissimilarity to that corresponding to Hoechst 33342. The similarity is that along with increasing the concentration of small molecule, the ion current

Table 1
Rectification ratios corresponding to three small biomolecules at transmembrane potential difference of 2 V.

Hoechst 33342 (μM)	Rectification ratio	Propidium iodide (μM)	Rectification ratio	Bupivacaine (μM)	Rectification ratio
0	4.80	0	5.4	0	5.2
2	2.09	20	3.62	400	4.07
3	0.43	200	2.40	3000	2.48
20	0.0079	1000	1.09	20,000	1.51

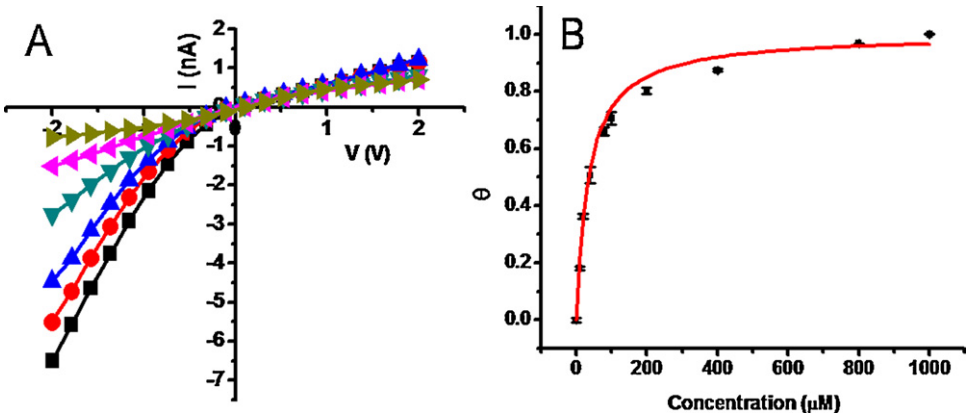

Fig. 4. (A) *I–V* curves for a conical nanochannel sensor (tip diameter = 22 nm, base diameter 200 nm) in the presence of the following concentrations of Propidium iodide: 0 nM (black square), 10 μM (red circle), 20 μM (blue triangle), 80 μM (green triangle), 400 μM (pink triangle), 1000 μM (dark yellow triangle). (B) Plot of surface coverage (theta) versus concentration of Propidium iodide. Red line is the fitting curve. Experimental conditions: 10 mM Tris buffer (pH = 7.0) with 100 mM in KCl; error bar from three experimental measurements. (For interpretation of the references to color in this figure legend, the reader is referred to the web version of the article.)

rectification gradually decreases. Nevertheless, the ion current rectification is not reversed at much high concentration of Propidium (Bupivacaine).

The similarity of molecular structures between Hoechst 33258 and Hoechst 33342 tell us that the interaction of Hoechst 33342 and nanochannel wall in PET can also be explained by hydrophobicity which was used to explain the interaction mechanism between Hoechst 33258 and nanochannel wall in Kapton [27]. Nonetheless, other weak forces like electrostatic interaction, hydrogen-bonding, aromatic stacking interaction, etc., still can not be fully ignored in this case. Electrostatic force is not the dominant force since Hoechst 33342 continue to be adsorbed onto the nanochannel wall after excess positive charge exists on the surface. For example, the less-than-unity ion current rectification indicates that the nanopore surface has net positive charge in the presence of 3 μM Hoechst 33342 (Table 1); increasing the concentration of Hoechst 33342 up to 20 μM can further decrease the ion current rectification, indicating that more molecules are absorbed. We reason that aromatic stacking interaction may play a significant role in the excessive adsorption of Hoechst 33342, which tends to aggregate due to its flat aromatic plane at high concentration. In contrary, Propidium and Bupivacaine do not have this capability, which may be used to explain why the ion current rectification is not reversed at high concentration.

3.4. Analysis of the small molecule adsorption data via Langmuir model

For Langmuir adsorption of a molecule to a surface, the following general equation was used [27]

$$\theta = \frac{KC}{1 + KC} \tag{1}$$

where θ is the fractional coverage of the molecule on the surface, K is the binding constant with units of L mol^{-1} and C is the concentration of the small molecule in the contacting solution phase. θ is also given by

$$\theta = \frac{\text{moles}_{s,i}}{\text{moles}_{s,\max}} \tag{2}$$

where $\text{moles}_{s,i}$ is the moles of molecule on the surface when the surface is exposed to some concentration of small molecule i and $\text{moles}_{s,\max}$ is the maximum adsorption capacity of the surface obtained at some very high concentration of the molecule.

At very high concentration of the molecule, the surface adsorption reached the maximum capacity and the corresponding ion current was referred to as $I_{\min}$; At the absence of the molecule, the ion current was I_0. $\text{Moles}_{s,\max}$ is proportional to the difference $I_0 - I_{\min}$.

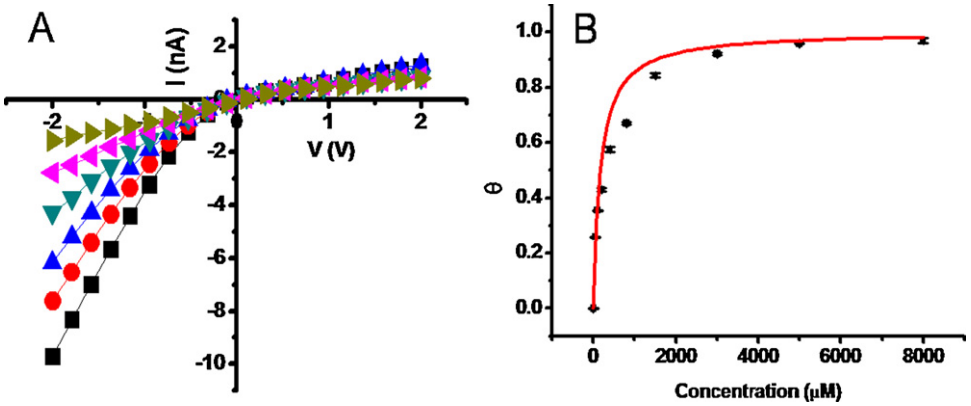

Fig. 5. (A) *I–V* curves for a conical nanochannel sensor (tip diameter = 22 nm, base diameter 200 nm) in the presence of the following concentrations of Bupivacaine: 0 nM (black square), 50 μM (red circle), 200 μM (blue triangle), 800 μM (green triangle), 1500 μM (pink triangle), 20,000 μM (dark yellow triangle). (B) Plot of surface coverage (theta) versus concentration of Bupivacaine. Red line is the fitting curve. Experimental conditions: 10 mM Tris buffer (pH = 7.0) with 100 mM in KCl; error bar from three experimental measurements. (For interpretation of the references to color in this figure legend, the reader is referred to the web version of the article.)

Similarly, if the current observed at some intermediate small molecule concentration was I_i, $moles_{s,i}$ is proportional to the difference $I_0 - I_i$. This allows us to calculate surface coverage for any concentration of small molecule via

$$\theta = \frac{I_0 - I_i}{I_0 - I_{min}} \quad (3)$$

By fitting the experimental data with Eq. (1), the value of the binding constant K can be obtained. Fig. 3B shows the experimental and calculated plots and a value of $K = 2.534 \times 10^6$ was obtained from the best fit. This K quantifies what the experimental data already taught us – Hoechst 33342 binds very strongly to the PET surface.

3.5. Fitting the experimental data with Langmuir model

Propidium and Bupivacaine are much less hydrophobic than Hoechst 33342. The first and second key experimental observations for Hoechst 33342 can be reproduced by Propidium and Bupivacaine (Table 1). As Propidium or Bupivacaine was added, the rectification was decreased (Figs. 4A and 5A); the rectification scaled inversely with the concentration of Propidium or Bupivacaine. The rectification was not reversed and still above unity even the concentration of Propidium or Bupivacaine was beyond 1 mM (Table 1). It meant that the surface charge of PET membrane had not been reversed even the maximum coverage of the small molecule was reached. Although Propidium have four aromatic rings, the tail attached to the ring could impede aromatic stacking interaction; Bupivacaine do not have planar molecular structure, which may prevent further adsorption via aromatic stacking.

Propidium was much more hydrophobic than Bupivacaine although there just has a slight difference in the molecular weights of Propidium and Bupivacaine. Bupivacaine presents two additional opportunities for hydrogen bonding with water: the lone pairs on the carbonyl group and the lone pair of the nonprotonated nitrogen. It was expected that the interaction between Bupivacaine and PET nanopore wall is the weakest one among the three small biomolecules. The bind constant (5.91×10^3 L/mol, Fig. 5B) for Bupivacaine to the nanochannel wall in PET membrane is lower than that for Propidium (2.85×10^4 L/mol, Fig. 4B) and that for Hoechst 33342 (2.53×10^6 L/mol, Fig. 3B).

The limit of detection (LOD) is defined as the concentration corresponding to the surface coverage at three times standard deviation of blank without analyte. The limit of quantification (LOQ) is defined as the concentration corresponding to the surface coverage at 10 times standard deviation of blank without analyte. For Hoechst 33342, the LOD and LOQ are 150 nM and 500 nM, respectively; for Propidium, the LOD and LOQ are 1.93 μM and 6.42 μM, respectively; For Bupivacaine, the LOD and LOQ are 6.33 μM and 21.1 μM, respectively. The highest binding constant is obtained for the small biomolecule with highest hydrophobicity. Another interesting result is that the detection limit for the small molecule with the highest binding constant shifts to submicromole.

4. Conclusions

The sensor we developed here has great selectivity toward hydrophobic cationic small biomolecules. More hydrophobic cationic small molecule can be easily discriminated from those less hydrophobic cationic small biomolecules. The highest binding constant of Hoechst 33342 toward nanochannel wall in PET membrane offers lowest detection limit. In the future work, we will focus on extend the application of sensor based on ion current rectification, for example, immobilize negative (or positive) charged molecular recognition agent onto the pore wall of conical nanotube for sensing positive (or negative) analytes.

Acknowledgements

This work was supported by National Natural Science Foundation of China (No. 20905056 and 21075120), the 973 Project (2009CB930100 and 2010CB933600).

References

[1] Z. Siwy, D. Dobrev, R. Neumann, C. Trautmann, K. Voss, Appl. Phys. A: Mater. Sci. Process. 76 (2003) 781–785.
[2] L.T. Sexton, L.P. Horne, C.R. Martin, Mol. BioSyst. 3 (2007) 667–685.
[3] L.T. Sexton, L.P. Horne, S.A. Sherrill, G.W. Bishop, L.A. Baker, C.R. Martin, J. Am. Chem. Soc. 129 (2007) 13144–13152.
[4] L.T. Sexton, H. Mukaibo, P. Katira, H. Hess, S.A. Sherrill, L.P. Horne, C.R. Martin, J. Am. Chem. Soc. 132 (2010) 6755–6763.
[5] F. Xia, W. Guo, Y.D. Mao, X. Hou, J.M. Xue, H.W. Xia, L. Wang, Y.L. Song, H. Ji, O.Y. Qi, Y.G. Wang, L. Jiang, J. Am. Chem. Soc. 130 (2008) 8345–8350.
[6] I. Lassiouk, T.R. Kozel, Z.S. Siwy, J. Am. Chem. Soc. 131 (2009) 8211–8220.
[7] M. Ali, B. Yameen, J. Cervera, P. Ramirez, R. Neumann, W. Ensinger, W. Knoll, O. Azzaroni, J. Am. Chem. Soc. 132 (2010) 8338–8348.
[8] M.L. Kovarik, K.M. Zhou, S.C. Jacobson, J. Phys. Chem. B 113 (2009) 15960–15966.
[9] M. Ali, B. Yameen, R. Neumann, W. Ensinger, W. Knoll, O. Azzaroni, J. Am. Chem. Soc. 130 (2008) 16351–16357.
[10] Y. He, D. Gillespie, D. Boda, I. Vlassiouk, R.S. Eisenberg, Z.S. Siwy, J. Am. Chem. Soc. 131 (2009) 5194–5202.
[11] Z. Siwy, L. Trofin, P. Kohli, L.A. Baker, C. Trautmann, C.R. Martin, J. Am. Chem. Soc. 127 (2005) 5000–5001.
[12] I. Vlassiouk, T.R. Kozel, Z.S. Siwy, J. Am. Chem. Soc. 131 (2009) 8211–8220.
[13] G.L. Wang, B. Zhang, J.R. Wayment, J.M. Harris, H.S. White, J. Am. Chem. Soc. 128 (2006) 7679–7686.
[14] R.J. White, E.N. Ervin, T. Yang, X. Chen, S. Daniel, P.S. Cremer, H.S. White, J. Am. Chem. Soc. 129 (2007) 11766–11775.
[15] B. Yameen, M. Ali, R. Neumann, W. Ensinger, W. Knoll, O. Azzaroni, J. Am. Chem. Soc. 131 (2009) 2070–2071.
[16] K.M. Zhou, M.L. Kovarik, S.C. Jacobson, J. Am. Chem. Soc. 130 (2008) 8614–8616.
[17] S.A. Miller, K.C. Kelly, A.T. Timperman, Lab Chip 8 (2008) 1729–1732.
[18] C.C. Harrell, Y. Choi, L.P. Horne, L.A. Baker, Z.S. Siwy, C.R. Martin, Langmuir 22 (2006) 10837–10843.
[19] R.J. White, B. Zhang, S. Daniel, J.M. Tang, E.N. Ervin, P.S. Cremer, H.S. White, Langmuir 22 (2006) 10777–10783.
[20] Y.B. Xie, J.M. Xue, L. Wang, X.W. Wang, K. Jin, L. Chen, Y.G. Wang, Langmuir 25 (2009) 8870–8874.
[21] E.A. Heins, Z.S. Siwy, L.A. Baker, C.R. Martin, Nano Lett. 5 (2005) 1824–1829.
[22] D. Krapf, M.Y. Wu, R.M.M. Smeets, H.W. Zandbergen, C. Dekker, S.G. Lemay, Nano Lett. 6 (2006) 105–109.
[23] A. Mara, Z. Siwy, C. Trautmann, J. Wan, F. Kamme, Nano Lett. 4 (2004) 497–501.
[24] Z.S. Siwy, M.R. Powell, A. Petrov, E. Kalman, C. Trautmann, R.S. Eisenberg, Nano Lett. 6 (2006) 1729–1734.
[25] S. Umehara, N. Pourmand, C.D. Webb, R.W. Davis, K. Yasuda, M. Karhanek, Nano Lett. 6 (2006) 2486–2492.
[26] M.Y. Wu, R.M.M. Smeets, M. Zandbergen, U. Ziese, D. Krapf, P.E. Batson, N.H. Dekker, C. Dekker, H.W. Zandbergen, Nano Lett. 9 (2009) 479–484.
[27] J. Wang, C.R. Martin, Nanomedicine 3 (2008) 13–20.
[28] Y. Astier, O. Braha, H. Bayley, J. Am. Chem. Soc. 128 (2006) 1705–1710.
[29] D. Wendell, P. Jing, J. Geng, V. Subramaniam, T.J. Lee, C. Montemagno, P.X. Guo, Nat. Nanotechnol. 4 (2009) 765–772.
[30] T.Z. Butler, M. Pavlenok, I.M. Derrington, M. Niederweis, J.H. Gundlach, Proc. Natl. Acad. Sci. U.S.A. 105 (2008) 20647–20652.
[31] H.C. Wu, Y. Astier, G. Maglia, E. Mikhailova, H. Bayley, J. Am. Chem. Soc. 129 (2007) 16142–16148.
[32] L.X. Zhang, X.H. Cao, Y.B. Zheng, Y.Q. Li, Electrochem. Commun. 12 (2010) 1249–1252.
[33] X. Hou, F. Yang, L. Li, Y.L. Song, L. Jiang, D.B. Zhu, J. Am. Chem. Soc. 132 (2010) 11736–11742.
[34] X. Hou, Y.J. Liu, H. Dong, F. Yang, L. Li, L. Jiang, Adv. Mater. 22 (2010) 2440–2443.
[35] X. Hou, W. Guo, F. Xia, F.Q. Nie, H. Dong, Y. Tian, L.P. Wen, L. Wang, L.X. Cao, Y. Yang, J.M. Xue, Y.L. Song, Y.G. Wang, D.S. Liu, L. Jiang, J. Am. Chem. Soc. 131 (2009) 7800–7805.
[36] M. Ali, V. Bayer, B. Schiedt, R. Neumann, W. Ensinger, Nanotechnology 19 (2008).
[37] C.C. Harrell, Z.S. Siwy, C.R. Martin, Small 2 (2006) 194–198.
[38] J.E. Wharton, P. Jin, L.T. Sexton, L.P. Horne, S.A. Sherrill, W.K. Mino, C.R. Martin, Small 3 (2007) 1424–1430.
[39] E.B. Kalman, O. Sudre, I. Vlassiouk, Z.S. Siwy, Anal. Bioanal. Chem. 394 (2009) 413–419.
[40] Z.S. Siwy, Adv. Funct. Mater. 16 (2006) 735–746.